BMC Microbiology

RESEARCH Open Access

Breed-specific differences of gut microbiota and metabolomic insights into fat deposition and meat quality in Chinese Songliao Black Pig and Large White × Landrace Pig Breeds

Suthar Teerath Kumar[1], Yunpeng Zhang[1], Qi Zhang[1,2], Riaz Muhammad Azeem[3], Zhang Jing[4], Li Pan[1], Wu-Sheng Sun[3*], Yuan Zhao[1*] and Shu-Min Zhang[1*]

Abstract

Background Gut microbiota ferment non-digestible substances to produce metabolites that accumulate in muscle and influence host metabolism. However, the regulatory mechanisms connecting gut microbiota, metabolites, and fat deposition across pig breeds remain unclear. This study explores the gut–muscle axis regulating fat deposition and meat quality in Chinese Songliao Black Pig (SBP) and Large White × Landrace Pigs (LWLDP). Digesta samples from the ileum, cecum, and rectum of both breeds were analyzed using 16 S rRNA sequencing for microbiome profiling and ultra-high-performance liquid chromatography (UHPLC) for metabolomics. Multi-omics data, including microbiota and metabolite profiles were integrated with our previously published data of transcriptomics and metabolomics insights into fat deposition in the *longissimus dorsi* (LD) muscle using the MixOmics DIABLO method.

Results Microbiome analysis revealed that *Fibrobacter*, *Unidentified_Peptostreptococcaceae*, *Sutterella*, and *Unidentifed_Rickettsiales* were enriched in SBP, while *Ruminococcus*, *Corynebacterium*, and *Streptococcaceae* in LWLDP. Metabolomic analysis indicated that SBP was enriched in fatty acid biosynthesis pathways, including linoleic acid, α-linolenic acid, and arachidonic acid, whereas LWLDP was associated with insulin signaling, starch and sucrose metabolism. Integrated analysis identified *Peptostreptococcaceae* and *Rickettsiales* in SBP, along with metabolites phosphatidylcholine (PC(22:4)), N-acylethanolamine (NAE(20:4)), and lysophosphatidylcholine (LysoPC(24:1)) were correlated with key genes (*EIF4E*, *MSTN*, *PPARGC1A*, *NR4A3*, *and SOCS1*) regulating fat deposition. In LWLDP, *Corynebacterium* and *Streptococcaceae* were linked to the *PPP1R3B* gene, which is involved in glycogen metabolism, as well as metabolites 2-methyl-3-hydroxybutyric acid and 5-keto-gluconic acid, suggesting a shift toward glycolysis over lipolysis.

*Correspondence:
Wu-Sheng Sun
sunwsh@jlau.edu.cn
Yuan Zhao
zhaoyuan4CL52@126.com
Shu-Min Zhang
shumin1961@126.com

Full list of author information is available at the end of the article

Conclusion This study concluded that cecum-associated microbes in LWLDP may enhance carbohydrate metabolism, leading to reduced fat deposition, whereas rectum-associated microbes in SBP contribute to *docosahexaenoic acid* (DHA) biosynthesis, thereby improving meat quality. These findings highlight gut microbiota-derived metabolites as potential biomarkers for optimizing meat production and livestock breeding strategies.

Keywords Fat deposition, Gut microbiomes, Gut–muscle axis, Meat quality, Metabolites, Pig breeds

Background

Fatty acids are key indicators of meat quality, playing a crucial role in the pig meat industry and significantly influencing overall consumer acceptability [1]. These are strongly linked to both nutrition and pork quality [2]. In recent decades, muscle fatty acid composition has been shown to be influenced by various factors, including heredity, age, diet, feeding environment, and gut microbiota. The gut microbiota is widely recognized for its role in regulating host metabolism, lipid absorption, and fat deposition in muscle tissues [3–5]. The gut harbors trillions of microorganisms that form complex communities [6]. They play a crucial role in host metabolism by fermenting non-digestible compounds and producing metabolites [7, 8]. Recent studies have shown that these gut microbes significantly influence growth performance [9], meat quality [10], and fatty acid composition [11, 12]. These metabolites can be affected by diet [13], environmental conditions [9], age [9, 14], and breed [15, 16], and they also vary among different regions of the intestine [17].

Gut microbes produce various classes of metabolites, such as bile acids, short-chain fatty acids such as butyrate, and vitamins, including thiamine, folate, biotin, riboflavin, and pantothenic acid, and the composition and microbial diversity of these metabolites are shaped by several factors, including genetics, age, sex, and diet [18]. These metabolites are produced through the combined act of the metabolic process of microorganisms and the host [19]. Metabolites encompass tangible compounds generated during the metabolic process, serving as both substrates and outcomes of metabolic reactions [20]. Metabolomics is a powerful analytical technique for comprehensively analyzing and comparing the end products of metabolic processes. It provides a detailed overview of metabolic profiles, linking metabolic pathways to their biological functions. Moreover, metabolomics offers insights into an organism's overall health by examining its complete metabolic network and investigating its processes in depth [21].

Numerous studies have investigated microbial composition across different intestinal regions, but most have been restricted to specific pig breeds [22–24]. Host genetics play a crucial role in shaping gut microbial communities across species [25]. Emerging research utilizing the MixOmics approach has demonstrated how gut microbiota-derived metabolites significantly influence fatty acid composition [11]. A recent breed-specific study revealed that microbiota derived from obese pigs can rewire carnitine metabolism, driving fatty acid deposition in the muscles of lean pig breeds [26]. Specific gut microbes—including *Bacteroides uniformis*, *Roseburia inulinivorans*, *Bacteroides vulgatus*, *Clostridium catus*, *Eubacterium rectale*, and *Faecalibacterium prausnitzii*—have been positively correlated with muscle metabolism-related genes (*MSTN*, *ATP2A1*, *MYLPF*, *ACTN3*, *MYL1*, and *TNNT3*), enhancing meat quality in cattle [27]. Similarly, the superior meat quality and higher intramuscular fat (IMF) content observed in Jinhua pigs has been linked to their gut microbiota. Mice transplanted with Jinhua pig microbiota exhibited increased lipid accumulation, triglyceride levels, and lipoprotein lipase activity, along with reduced *ANGPTL4* expression in muscle [28]. Another study reported a higher *Firmicutes/Bacteroidetes* ratio and greater abundance of *Romboutsia* and *Prevotella copri* in pigs, suggesting a role in fat accumulation via TLR4 and mTOR pathways. This study also showed upregulation of lipogenesis-related genes (*Fabp9*, *Scd1*, *Scd2*, *and Scd3*), further supporting the influence of gut microbes on fat deposition and meat quality [29]. These findings collectively suggest that gut microbiota significantly impact meat quality through modulation of muscle gene expression. However, substantial breed-specific variations exist in fatty acid composition and meat quality, and the molecular mechanisms underlying these differences—particularly the role of gut microbiota and their metabolic pathways in fat deposition remain poorly understood.

Our previous study investigated the transcriptome and metabolome insights into key genes regulating fat deposition and meat quality in Chinese Songliao Black Pigs (SBP) and Large White × Landrace pigs (LWLDP) [30]. Building on these findings, this study aims to elucidate the role of the gut microbiota and its metabolites in regulating the molecular mechanisms underlying fat deposition and meat quality in pig breeds. Specifically, we aimed to (1) Investigate breed-specific differences in gut microbiota composition and metabolite profiles across distinct intestinal regions (ileum, cecum, and rectum). (2) Integrate gut microbiota and metabolite with our previous transcriptomic and muscle metabolite study to identify microbial taxa and metabolites associated with fat deposition and meat quality. This research seeks to advance

understanding of the gut–muscle axis in pigs, potentially providing biomarkers for improved meat quality.

Methods

Study site, animals and experimental design

A total of one hundred male pigs (fifty Songliao Black Pigs (SBP) and fifty Large White × Landrace pigs (LWLDP)) were reared at Gongzhuling National Agricultural Science and Technology Park (Feimas Animal Husbandry Co., Ltd., Gongzhuling, China) under uniform conditions. All animal procedures were approved by the Institutional Animal Care and Use Committee (IACUC) of Jilin Agricultural University (approval number KT2023023). Clinical trial number: not applicable. Pigs were reared under pen housing with same feeding management, diet composition, and environmental conditions. At an average age of 210 ± 15 days, the pigs were transported to Gongzhuling Gaojin Food Co., Ltd. for slaughtering. Live weight was recorded before humane euthanasia by electric shock, followed by rapid exsanguinations. *Longissimus dorsi* (LD) muscle samples were collected for fatty acids, amino acids profiling, transcriptomics, metabolomics and meat quality assessment,, as published in our previous study [30]. At the similar time, digesta samples were collected from the ileum, cecum, and rectum by opening the respective sections of the intestines of both breeds. The samples were immediately transferred into sterile 7 ml cryopreservation tubes and snap-frozen in liquid nitrogen to preserve microbial and metabolic integrity. These frozen samples were subsequently stored at − 80 °C for storage until further analysis. Similar samples were used for microbial diversity analysis and metabolite profiling, as mentioned in our earlier study. The breed-specific comparison and integration of multi-Omics data for exploring the strong association between the gut and muscle axes regulating fat deposition and meat quality in pig breeds were followed a similar method of MixOmics Diablo analysis for the integrated analysis of multiple types of Omics data, as explained by [31].

Detection of intestinal metabolites

Five digesta samples from each intestinal segment (ileum, cecum and rectum) of both breeds were taken for metabolite detection, as described by [32]. Polar metabolites were analyzed via a UHPLC system (Vanquish, Thermo Fisher Scientific, Waltham, MA, USA) with a Waters ACQUITY UPLC BEH amide column (2.1 mm × 50 mm, 1.7 µm) connected to an Orbitrap Exploris 120 mass spectrometer (Thermo Fisher Scientific, Waltham, MA, USA). The mobile phase included 25 mmol/L ammonium acetate and 25 mmol/L ammonium hydroxide in water (pH 9.75) as phase A and acetonitrile as phase B. The autosampler was kept at 4 °C, and 2 µL of sample was injected. The mass spectrometer was operated in information-dependent acquisition (IDA) mode, with control via Xcalibur software (Thermo Fisher Scientific, Waltham, MA, USA). The electrospray ionization (ESI) parameters used were as follows: sheath gas flow rate of 50 Arb, auxiliary gas flow rate of 15 Arb, capillary temperature of 320 °C, full MS resolution of 60,000, MS/MS resolution of 15,000, stepped normalized collision energy (SNCE) of 20/30/40, and spray voltages of 3.8 kV (positive mode) or -3.4 kV (negative mode).

Analysis of intestinal metabolites

Untargeted metabolite analysis was performed via total ion chromatograms (TICs). The raw data for both positive and negative ion metabolite concentrations were processed with XCMS software [33], which manages peak alignment, retention time correction, and peak area extraction. Following data processing with XCMS, metabolite identification and data preprocessing were carried out [34]. Multivariate statistical analyses, including principal component analysis (PCA), partial least squares discriminant analysis (PLS-DA), and orthogonal partial least squares discriminant analysis (OPLS-DA), were conducted via the R package Ropls [35]. Differential expressed metabolite (DEM) analysis was performed with a significance threshold of$|Log2Fc| > 1$ and an adjusted p value < 0.05 [36]. A volcano plot and a cluster heatmap were generated to visualize the results [37]. The Kyoto Encyclopedia of Genes and Genomes (KEGG) database was used to analyze the differentially expressed metabolic pathways [38].

DNA extraction and high-throughput sequencing

Five digesta samples from each intestinal region (ileum, cecum, and rectum) of both breeds, with two replicates for each sample were used for microbial analysis. Total genomic DNA was extracted via an Omega soil DNA kit (M5635-02) (Omega Bio-Tek, Norcross, GA, USA). The quantity and quality of the extracted DNA were measured via a NanoDrop NC2000 spectrophotometer (Thermo Fisher Scientific, Waltham, MA, USA) and agarose gel electrophoresis, respectively. PCR amplification of the bacterial 16 S rRNA gene V3–V4 region was performed via the forward primer 338 F (5'-ACTCCTA CGGGAGGCAGCA-3') and the reverse primer 806R (5'-GGACTACHVGGGTWTCTAAT-3'). Sample-specific 7-bp barcodes were incorporated into the primers for multiplex sequencing. The PCR components included 5 µl of 5× reaction buffer, 0.25 µl of Fast Pfu DNA Polymerase (5 U/µl), 2 µl of dNTP mixture (2.5 mM each), 1 µl of each forward and reverse primer (10 µM), 1 µl of the DNA template, and 14.75 µl of nuclease-free water (dd-H_2O). Thermal cycling consisted of initial denaturation at 98 °C for 5 min, followed by 25 cycles consisting

of denaturation at 98 °C for 30 s, annealing at 53 °C for 30 s, and extension at 72 °C for 45 s, with a final extension of 5 min at 72 °C. The PCR amplicons were purified with Vazyme VAHTSTM DNA Clean Beads (Vazyme, Nanjing, China) and quantified via the Quant-iT PicoGreen dsDNA Assay Kit (Invitrogen, Carlsbad, CA, USA). After the individual quantification step, amplicons were pooled in equal amounts, and pair-end 2 × 250 bp sequencing was performed via the Illumina NovaSeq platform with a NovaSeq 6000 SP Reagent Kit (500 cycles) at Shanghai Personal Biotechnology Co., Ltd. (Shanghai, China).

Bioinformatics analysis

The raw 16 S rRNA sequence data were analyzed via the QIIME2 and R packages (v3.2.0) [39]. Alpha diversity indices (Chao1, observed species, Shannon, Simpson, Faith's PD, Pielou's evenness, and Good's coverage) were calculated from the ASV table in QIIME2 and visualized as box plots. Beta diversity analysis was used to assess microbial community structure variation via Jaccard, Bray–Curtis, and UniFrac distance metrics, which were visualized through principal coordinate analysis (PCoA). Significance in microbiota structure differentiation was assessed via permutational multivariate analysis of variance (PERMANOVA) conducted via QIIME2. Taxonomic compositions and abundances were visualized with MEGAN and GraPhlAn. Differentially abundant taxa were identified via linear discriminant analysis effect size (LEfSe) [39]. Orthogonal partial least squares discriminant analysis (OPLS-DA) was performed with the R package Muma [40]. Microbial functions were predicted via PICRUSt2 and MetaCyc [41] and KEGG databases (http://www.genome.jp/kegg/).

Key genes analysis of DHA fatty acids

In our previous study, Pearson correlation analysis between differentially expressed genes (DEGs) and DHA fatty acid levels was performed via the Hmisc R package [35, 42]. The genes exhibiting a significant correlation ($p < 0.05$, $r > 0.7$) between DHA and DEGs were selected for further analysis. The STRING database was used to construct a protein–protein interaction (PPI) network for these genes. Subsequently, cytoHubba plugin of Cytoscape software (v3.10.2) was used to identify the top 10 hub genes characterized by the highest degree of connectivity within the network [30].

Integrated mixomics analysis

The integration of significant microbial taxa, predicted microbial KO pathways, top 15 up- and down-regulated intestinal metabolites of ileum, cecum and rectum region along with *longismuss dorsi* muscle metabolites were selected based on (log2FC > ± 1 and p value < 0.05), and genes regulating fat deposition and meat quality in pig breeds was integrated via the DIABLO framework from the MixOmics (v 6.25.1) R package [43]. The LD muscle metabolites and key genes regulating fat deposition and meat quality were selected from our previous study [30]. Initially, a DIABLO model was constructed via the sPLS-DA correlation function to establish relationships between multiple Omics data blocks. Various visualization techniques, including Circos plots, correlation circle plots based on CCA analysis and cluster image maps (CIMs) plots, were subsequently designed to explore the relationships and interactions between blocks at a correlation threshold of 0.8 for strong associations. We followed a similar method as explained by [31].

Statistical analysis

The relative abundance of taxa at the genus level and the predicted microbial metabolic pathways were compared via *Student's t test* in SPSS version 26 (IBM Corp., Armonk, NY, USA). The significant differences between the SBP and LWLDP breeds were evaluated, with a p value < 0.05 considered statistically significant. Additionally, correlations between intestinal metabolites, significant taxa, and significant microbial KEGG Orthology (KO) pathways were analyzed via the Pearson correlation method implemented with the Hmisc R package. The results were visualized via the Pheatmap package [35, 42].

Results

Differentially expressed metabolites (DEMs) and functional analysis

Untargeted metabolomic analysis revealed an average of 18,089 metabolites in each intestinal section (ileum, cecum, and rectum), detected metabolites are shown in (Additional file S1). Multivariate analyses revealed distinct metabolic profiles between SBP and LWLDP pigs, and principal component analysis (PCA) indicated significant variations across intestinal regions in both breeds (Fig. 1A). Orthogonal partial least squares discriminant analysis (OPLS-DA) identified 2,183 metabolites commonly expressed across all the intestinal sections. In the ileum, 38 differentially expressed metabolites (DEMs) were identified (Fig. 1B), with 30 up-regulated in LWLDP pigs and 8 down-regulated in SBP pigs detailed in (Additional file S2). In the cecum, 42 DEMs were detected, 32 of which were up-regulated in LWLDP and 10 of which were down-regulated in SBP (Fig. 1C) and detailed in (Additional file S3). Analysis of the rectum revealed 75 DEMs (Fig. 1D), including 15 up-regulated and 63 down-regulated metabolites detailed in (Additional file S4). The metabolite distributions of SBP and LWLDP in samples from the ileum, cecum and rectum are shown in (Fig. 1E).

Functional analysis of ileum, cecum, and rectum metabolites revealed different metabolic pathways in SBP and LWLDP pigs. In the ileum, the fatty acid biosynthesis

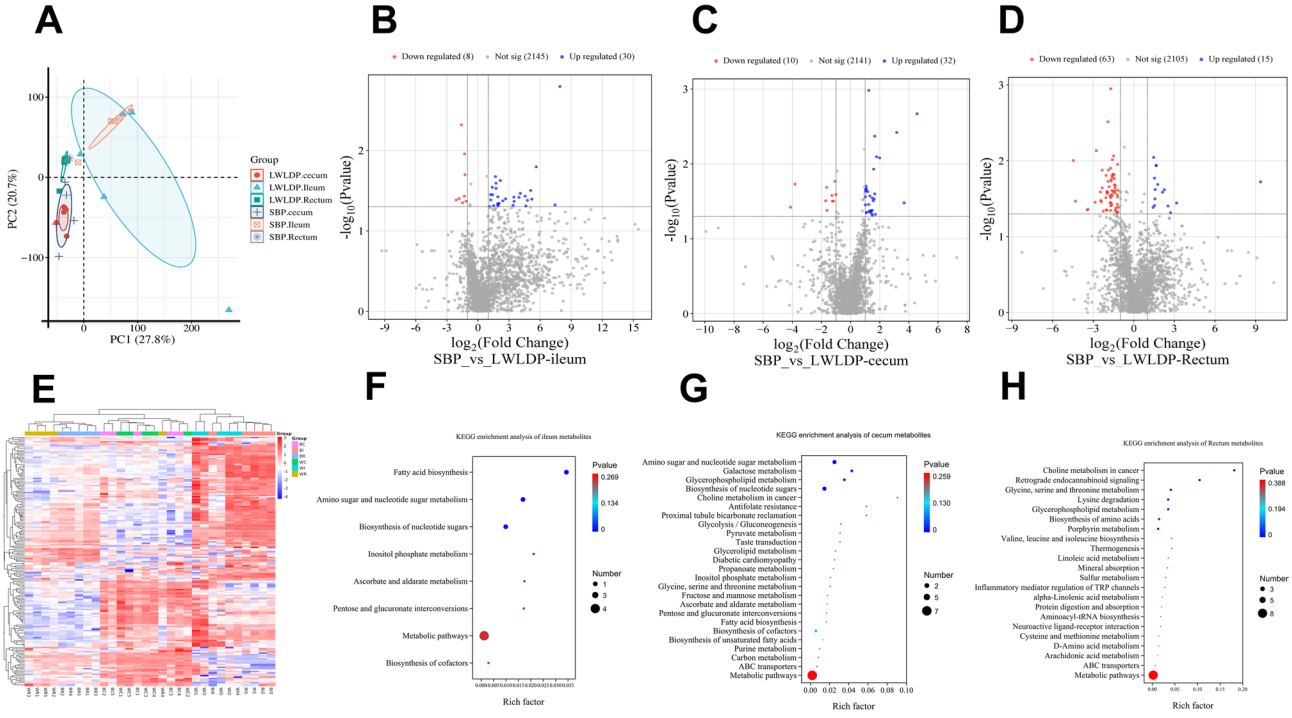

Fig. 1 Intestine metabolites analysis **(A)** Principle component analysis of ileum, cecum and rectum region metabolites of SBP and LWLDP pigs breeds **(B)** Differential expressed metabolite analysis of ileum region **(C)** Differential expressed metabolite analysis of Cecum region **(D)** Differential expressed metabolite analysis of Rectum region **(E)** Differential expressed metabolite distribution in samples of ileum, cecum and rectum of SBP and LWLDP **(F)** KEGG pathways of ileum region metabolites **(G)** KEGG pathways of cecum region metabolites **(H)** KEGG pathways of rectum region metabolites

pathway down-regulated capric acid and cis-9-palmitoleic acid metabolites in SBP pigs, which may have contributed to altered fat deposition patterns compared with those in LWLDP pigs. Amino sugar and nucleotide sugar metabolism, as well as the biosynthesis of nucleotide sugars, was up-regulated in glucuronic acid and N-acetylmuramic acid in LWLDP pigs. These metabolites could influence collagen biosynthesis and, consequently, meat tenderness. Additionally, inositol phosphate metabolism and ascorbate and aldarate metabolism were associated with the up-regulation of glucuronic acid in LWLDP pigs (Fig. 1F) detailed in (Additional file S5). In the cecum, amino sugar and nucleotide sugar metabolism, which are central to carbohydrate and lipid metabolism, was up-regulated in glucuronic acid, glucose, and galactose in LWLDP pigs. These changes could reflect altered metabolic activity influencing fat deposition in the LD muscle. The glycerophospholipid metabolism pathway was enriched with sn-glycerol 3-phosphate and sn-glycerol 1-phosphate in LWLDP pigs, suggesting that modifications in the phospholipid content may affect fat cell composition and storage capacity (Fig. 1G), and detailed in (Additional file S6) In the rectum, the retrograde endocannabinoid signaling pathway included metabolites such as NAE (20:4) (AEA) and PC (16:0/16:1(9Z)) in SBP, indicating their involvement in neural signaling and lipid-based signaling mechanisms. Additionally, glycine, serine, and threonine metabolism involves metabolites such as threonine and homoserine, which are essential for amino acid and protein biosynthesis. The lysine degradation pathway involves 5-hydroxylysine, a metabolite linked to protein modification and collagen stability. In lipid metabolism, linolenic acid metabolism, alpha linolenic acid and arachidonic acid are associated with significant metabolites such as PC (20:3(5Z,8Z,11Z)/14:0), PC (18:0/18:3(6Z,9Z,12Z)), PC(22:4(7Z,10Z,13Z,16Z)/P-18:1(9Z)), PC(14:1(9Z)/P-18:0), PC(20:2(11Z,14Z)/18:3(9Z,12Z,15Z)), and LysoPC(24:1(15Z)) in SBP, which may impact fat composition and muscle fat deposition in the LD muscle (Fig. 1H), detailed in (Additional file S2). Overall, the analysis underscores the pivotal role of carbohydrate, lipid, and amino acid metabolism pathways in regulating fat deposition and influencing meat quality traits.

Comparative analysis of the gut microbiota

The raw 16 S rRNA sequencing data of the ileum, cecum, and rectum samples were subjected to filtering, denoising, merging, and removal of chimeric and singleton sequences to ensure high-quality data for comparative analysis between the Songliao black pig (SBP) and LWLDP breeds, as detailed in (Additional file S8). A total of 28,283 to 66,113 high-quality non-singleton reads per sample were retained, providing sufficient

sequencing depth for robust microbial community analysis. Notably, the ileum in both breeds presented the least sequence reduction, with LWLDP maintaining higher sequence counts across all the intestinal sections. Alpha diversity metrics revealed that LWLDP had greater microbial diversity in the cecum and rectum, whereas the ileum displayed similar diversity levels between the two breeds (Fig. 2A). In contrast, β diversity analysis via the Bray–Curtis distance clearly distinguished the microbial composition between the intestinal sections of SBP and LWLDP (Fig. 2B). The relative abundance analysis revealed that, compared with SBP pigs, LWLDP pigs presented greater microbial abundances across all intestinal sections. A cladogram with an LDA threshold of 3 identified for differences in microbial taxa between the two breeds. Interestingly, SBP was associated with greater microbial diversity, particularly in the rectum (Fig. 2C-D). At the phylum level, *Firmicutes*, *Bacteroidetes*, *Proteobacteria*, and *Spirochaetes* were the most prevalent phyla across both breeds (Fig. 2E). At the family level, *Lactobacillaceae*, *Ruminococcaceae*, *Streptococcaceae*, *Paraprevotellaceae*, and *S24-7* were dominant (Fig. 2F). At the genus level, *Lactobacillus*, *Streptococcus*, *Prevotella*, and *YRC22* were prominent (Fig. 2G). At the species level, *Lactobacillus reuteri*, *Prevotellacopri*, *Streptococcus luteciae*, and *Lactobacillus mucosae* were identified as the most abundant taxa in both breeds (Fig. 2H).

Identification of significant taxa and predicted microbial KO pathways in different regions of the intestine

The relative abundance analysis of taxa at the genus level and the predicted abundance scores for microbial metabolic pathways across regions in both breeds revealed distinct microbial profiles. We found no significant differences in the ileum between the breeds. However, nine bacterial genera were significantly abundant in the cecum. In SBP, *Fibrobacter* and *unclassified Betaproteobacteria* were significantly more abundant ($p < 0.05$). In contrast,

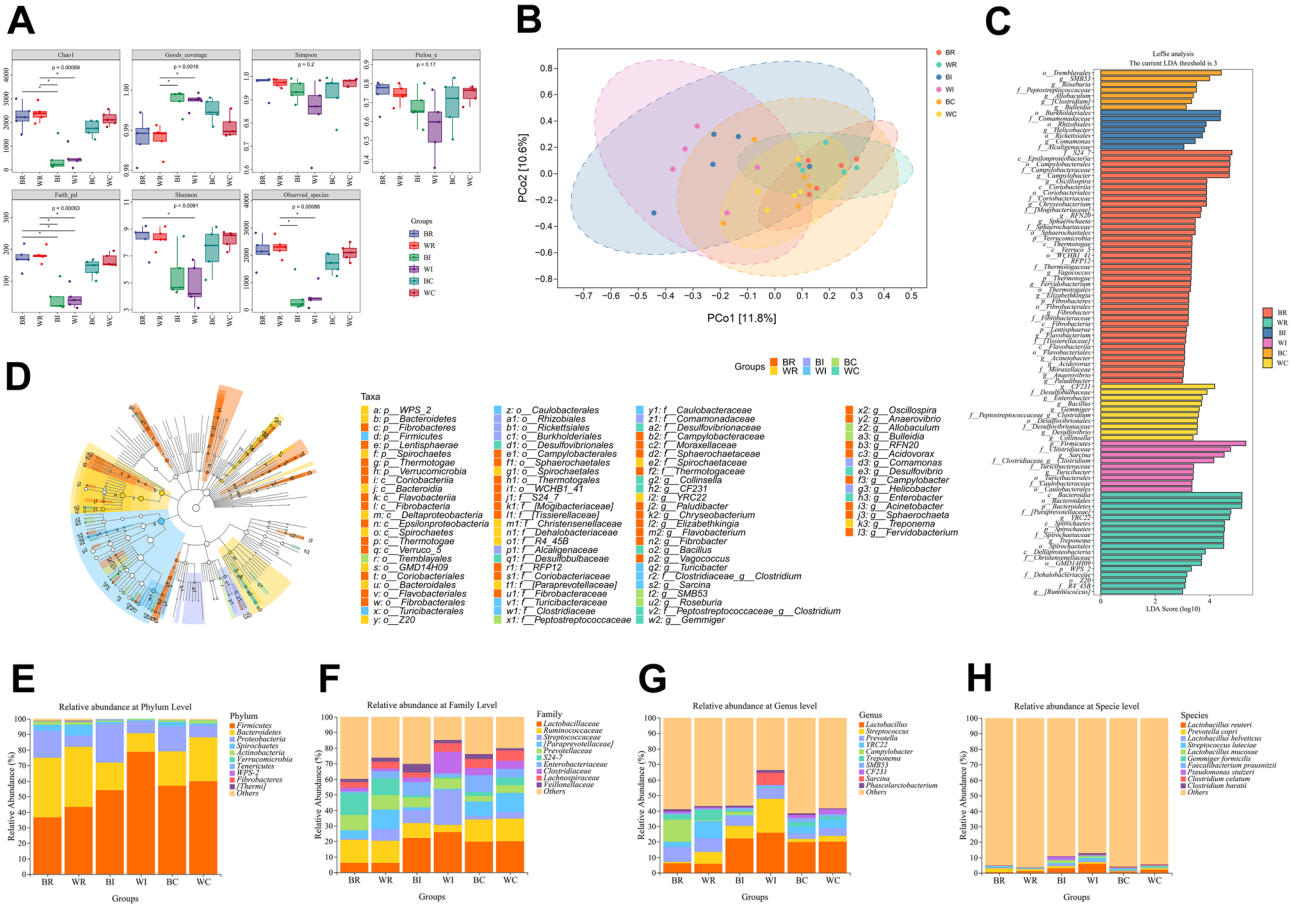

Fig. 2 Comprehensive microbial analysis of intestinal samples from SBP and LWLDP pig breeds. **(A)** Alpha diversity analysis indices insights into the diversity of microbial communities in the ileum, cecum, and rectum across both pig breeds. **(B)** Beta diversity analysis using Bray-Curtis distance, depicting distinct clustering of microbial communities between the ileum, cecum, and rectum. **(C-D)** LEfSe (Linear Discriminant Analysis Effect Size), displaying bacterial taxa with varying abundance between ileum, cecum and rectum of SBP and LWLDP breeds at LDA threshold of 3 for taxons contributing to microbial community differences. **(E)** Relative abundance at phylum level **(F)** relative abundance at family level **(G)** relative abundance at genus level **(H)** relative abundance at species level

LWLDP had higher abundances of *Corynebacterium and Desulfovibrio* ($p < 0.001$), *unclassified Streptococcaceae* ($p < 0.01$), *Bacillus*, *unclassified RFP12*, *unclassified Firmicutes*, and *Enterobacter* ($p < 0.05$). In the rectum, five genera were significantly different; four of these *unclassified Peptostreptococcaceae* ($p < 0.001$), *unclassified Rickettsiales* ($p < 0.01$), and *Sutterella* ($p < 0.05$) were more abundant in SBP, whereas *Ruminococcus* ($p < 0.05$) was significantly enriched in LWLDP (Fig. 3A). The analysis of the predicted microbial metabolic pathways revealed no significant differences in the ileum. However, in the cecum region, four significant pathways, such as systemic lupus erythematosus ($p < 0.001$), starch and sucrose metabolism, and sphingolipid metabolism ($p < 0.05$), were significantly more abundant in LWLDP, whereas the ABC transporter pathway ($p < 0.01$) was more enriched in SBP. In the rectum, the insulin signaling pathway ($p < 0.01$), porphyrin and chlorophyll metabolism, and plant hormone signal transduction ($p < 0.05$) were more abundant in LWLDP. In contrast, ascorbate and aldarate metabolism, atrazine degradation, lysine degradation, glycophospholipid metabolism, biotin metabolism, linoleic acid metabolism, and carotenoid biosynthesis ($p < 0.05$) were significantly more common in SBP (Fig. 3B).

Key genes associated with DHA fatty acids

The DEGs correlated with DHA fatty acid levels ($r > 0.7$, $p < 0.05$) were identified, as reported in our previous study [30]. A total of 97 genes exhibiting significant correlations with DHA were selected for further analysis, more detailed in (Additional file S9). Functional analysis of these genes was performed through protein–protein interaction (PPI) network construction. From the PPI network, the top 10 hub genes (*IL6*, *PTGS2*, *ICAM1*, *THBS1*, *MYC*, *PTX3*, *TNFAIP6*, *PLAU*, *ATF3*, *and SOCS3*) were identified on the basis of their high degree of connectivity and interactions with other genes. These hub genes represent key regulatory factors modulated by the fatty acid DHA and may play critical roles in associated metabolic and biological processes.

Correlation analysis of intestinal microbes and predicted functional microbial KO pathways

Pearson correlation of bacterial genera and microbial KO pathways revealed significant associations (Fig. 4). *Firmicutes* was positively associated with sphingolipid, starch, and sucrose metabolism and negatively associated with the ABC transporter. *Bacillus* was positively correlated with the systemic lupus erythematosus pathway. *Corynebacterium* was positively associated with starch and sucrose metabolism. *Streptococcaceae* was positively correlated with plant hormone signal transduction and starch and sucrose metabolism but negatively correlated with ABC transporters and lysine degradation. Moderate positive correlations were observed for *Ruminococcus* with plant hormone signaling and starch and sucrose metabolism. *Desulfovibrio* and *RFP12* were positively correlated with the insulin signaling pathway, whereas *Fibrobacter* was associated with porphyrin and chlorophyll metabolism. *Unidentified_Rickettsiales* was positively correlated with lysine degradation, carotenoid biosynthesis, and the ABC transporters. *Unidentifed_Peptostreptococcaceae* was negatively correlated with starch and sucrose metabolism, whereas *Sutterella* was positively associated with linoleic acid metabolism, atrazine degradation, and glycerophospholipid metabolism

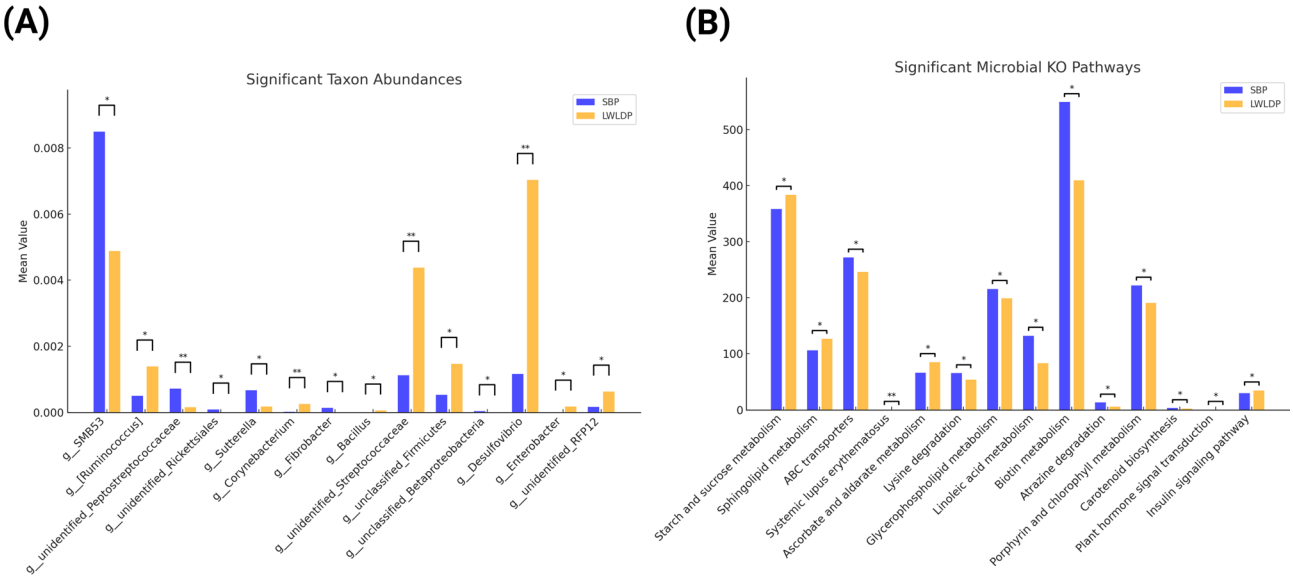

Fig. 3 Significant taxon and microbial KO pathways in different region of intestine of SBP and LWLDP pig breeds **(A)** Significant taxon in different regions of intestine of SBP and LWLDP **(B)** Significant microbial KO pathways in different regions of intestine of SBP and LWLDP

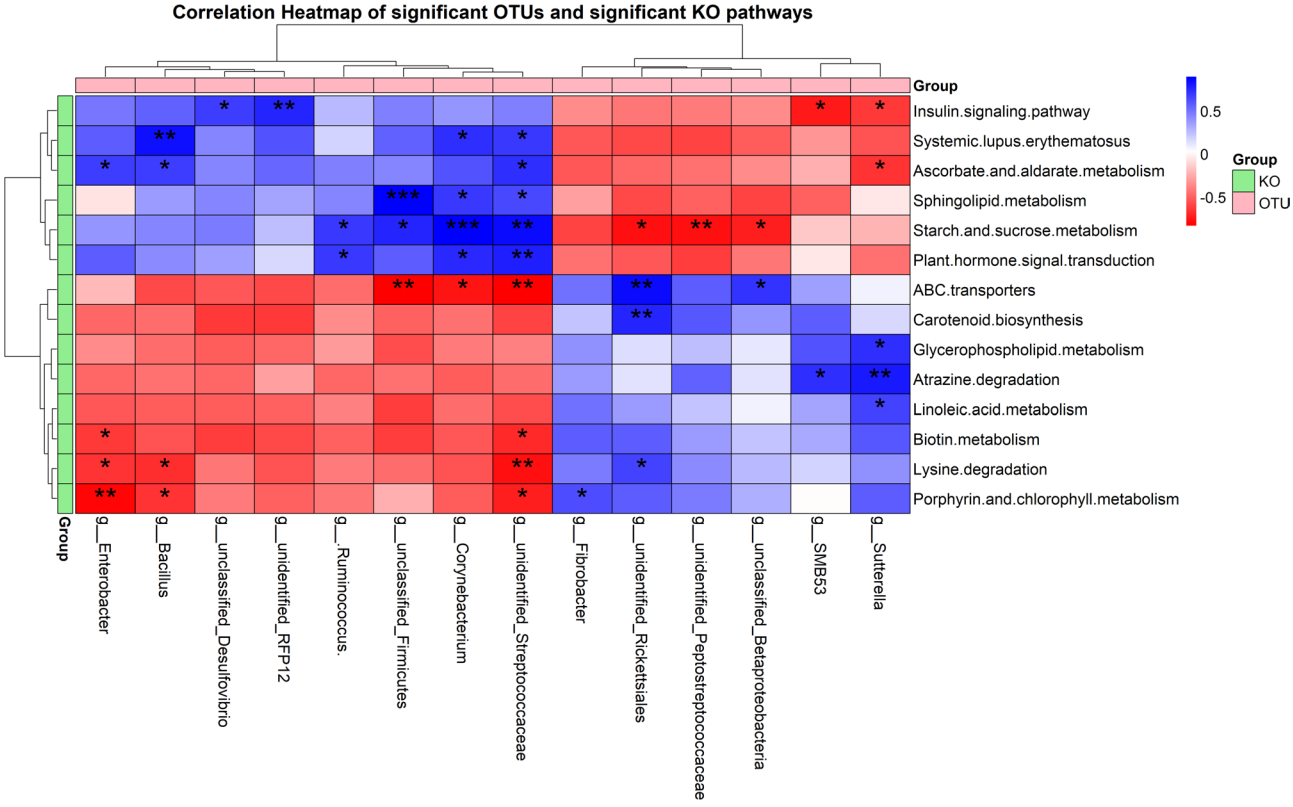

Fig. 4 Pearson correlation analysis between significant taxa at genus level and significant microbial functional KO pathways of ileum, cecum and rectum of SBP and LWLDP pig breeds

and negatively associated with the insulin signaling pathway and ascorbate and aldarate metabolism.

Correlation analysis of significant taxa and intestinal metabolites

Pearson correlations of significant microbial taxa and highly up- and down-regulated metabolites in the ileum, cecum and rectum regions revealed notable interactions (Fig. 5). In the ileum, the *g_SMB53* genus showed strong positive correlation with cis-9-palmitoleic acid, M1549.neg and 1-palmitoyl-2-docosahexaenoyl-sn-glycero-3-phospho-(1'-rac-glycerol) but strongly negatively correlated with apigenin 6,8-digalactoside. *Sutterella* was strong positively correlated with M1215.neg. *Unidentified_Rickettsiales* were highly positively correlated with PC (P-18:0/18:1(9Z)). *Unclassified_Desulfovirio* were strongly correlated with apigenin 6,8-digalactoside and 3-[(ethylanilino)methyl] benzenesulfonic acid but negatively correlated with cis-9-palmitoleic acid, 2-hydroxy-2',3'-dichlorobiphenyl, M1549.neg and (24E)-12,15-dihydroxy-3-(pentopyranosyloxy)-9,19-cyclolanost-24-en-26-oic acid. *Ruminococcus* was moderately significantly correlated with most of the regulated metabolites. In the cecum, *Sutterella* was strongly positively correlated with inosine 5'-monophosphate (IMP), M1753.pos, N-oleoyltaurine, M1712.pos, gabapentin, PC (P-16:0/0:0) and M1403.pos but moderately negatively correlated with N-benzyladenine and 4-phenoxy-N-(2-pyridinylmethyl) benzamide. *Fibrobacter* was highly positively correlated with 10-formyldihydrofolate. *Bacillus*, *Corynebacterium*, *Unidentified_Streptococcaceae* and *Firmicutes* were strongly correlated with 2-methylbutylamine. *Ruminococcus* was highly positively correlated with 5-Keto-Gluconic acid, 2-(4-Benzoyl-3-hydroxyphenoxy) ethyl acrylate, 4-Nitrophenol, ZON, M1843.neg, Dehydrogriseofulvin, N-Acetylgalactosamine_6-sulfate and Isoferulic acid but negatively correlated with (2,2,3,3-Tetrafluoropropoxy) acetic acid. In the rectum, *Enterobacter* was highly positively correlated with 2-methyl-3-hydroxybutyric acid, sterebin D, 3-(dodecylsulfonyl) propanoic acid and Phe-(benzyloyl)-Leu-Arg, whereas *Bacillus* was strongly positively correlated with 16-oxopalmitate and 7-oxopimara-8(14),15-dien-20-oic acid. *Corynebacterium* was strongly positively correlated with 3-[(3-carboxypropanoyl)amino]benzoic acid, 7-oxopimara-8(14),15-dien-20-oic acid and 5-(2-furyl)-1,3,4-oxadiazole-2(3 H)-thione but negatively correlated with 2-(1,4,5,7-tetramethyl-6 H-pyrrolo[3,4-d] pyridazin-6-yl) aniline. *Unidentified_Streptococcaceae* were strongly correlated with 7-oxopimara-8(14), 15-dien-20-oic acid, erythronolactone

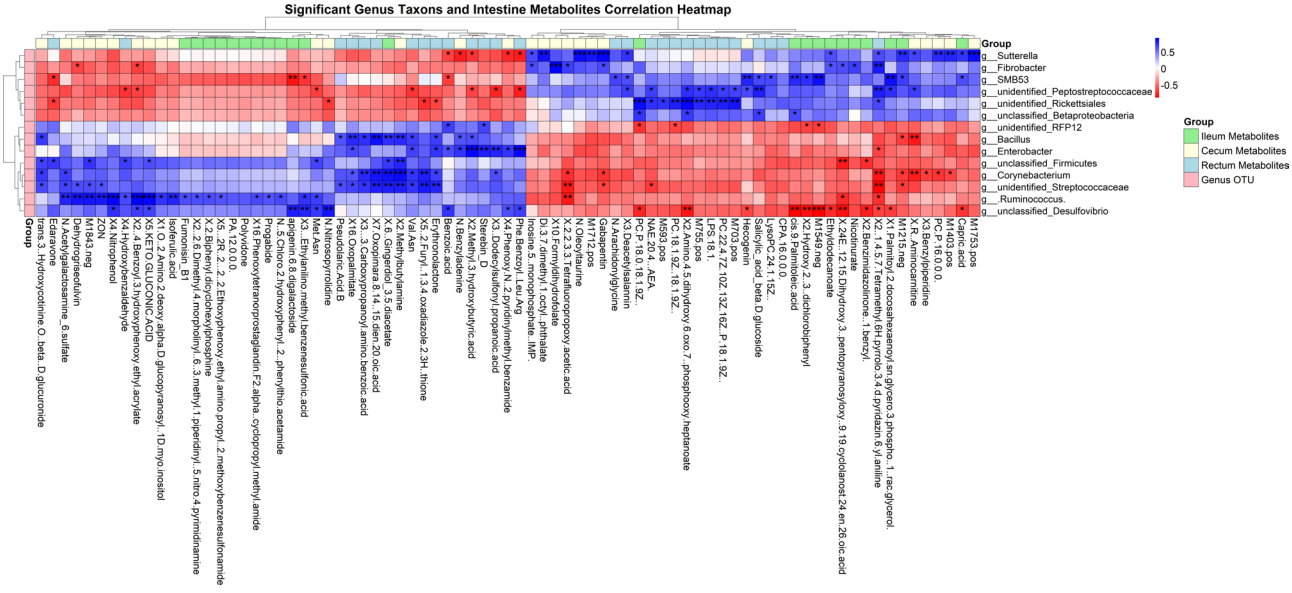

Fig. 5 Pearson correlation analysis of highly up-regulated and down-regulated metabolites of ileum, cecum and rectum metabolites with significant taxa at genus level of SBP and LWLDP pig breed

and 5-(2-furyl)-1,3,4-oxadiazole-2(3 H)-thione but strongly negatively correlated with 2-(1,4,5,7-tetramethyl-6 H-pyrrolo[3,4-d] pyridazin-6-yl) aniline. *Unidentified_-Peptostreptococcaceae* were strongly correlated with salicylic acid beta-D-glucoside and 2-(1,4,5,7-tetramethyl-6 H-pyrrolo[3,4-d] pyridazin-6-yl) aniline. *Unidentified Rickettsiales* were strongly correlated with PC (18:1(9Z)/18:1(9Z)), 2-Amino-4,5-dihydroxy-6-oxo-7-(phosphooxy) heptanoate, M755.pos, LPS (18:1), PC (22:4(7Z,10Z,13Z,16Z)/P-18:1(9Z)) and LysoPC (24:1(15Z)).

Integrated mixomics analysis

Initially, a DIABLO model was created via the sPLS-DA method to explore the correlations between multiple Omics datasets from the gut and muscles (Fig. 6A). Positive and negative correlations among variables across the mixomics blocks were visualized in a Circos plot with a cutoff of 0.8 (Fig. 6B). Based on the multi-Omics molecular signature expression for each sample, the ten samples were clustered into two classes, consistent with the beed group to which they belonged (Fig. 6C). Data integration revealed that key genes—*ATF3*, *EIF4E*, *ICAM1*, *PLAU*, *IL6*, *PTX3*, *MSTN*, *PPARGC1A*, *SOCS3*, *NR4A3*, *PTGS2*, *SOCS1*, *THBS1*, *MYC*, *INHBB*, and *TNFAIP6*—regulate fat deposition and meat quality. Microbial taxa, including *Unidentified_Peptostreptococcaceae* and *Unidentifed_Rickettsiales*, were associated with lysine degradation, biotin metabolism, linoleic acid metabolism, and predicted orthologous KO pathways. Intestinal metabolites, including PC (22:4(7Z,10Z,13Z,16Z)/P-18:1(9Z)/P593.pos), NAE (20:4) (AEA), and LysoPC(24:1(15Z)) in the ileum; gabapentin in the cecum; and 2-benzimidazolinone, 1-benzyl-, cis-9-palmitoleic acid, (24E)-12,15-dihydroxy-3-(pentopyranosyloxy)-9,19-cyclolanost-24-en-26-oic acid, 2-hydroxy-2',3'-dichlorobiphenyl, and ethyldodecanoate metabolites in the rectum; and 5-methoxycarbonylamino-N-acetyltryptamine, Sotalol, M967.neg, 2-(aminomethyl)-4-(tert-butyl)-6-(methyl sulfonyl)phenol, 7-methoxycoumarin-4-acetic acid, and 2-(1,4,5,7-tetramethyl-6 H-pyrrolo[3,4-d]pyridazin-6-yl) aniline, which are metabolites of LD muscle in SBP. These findings highlight the correlations between the gut and muscles, underscoring the complex metabolic activity of SBP and offering new insights into the unique regulatory mechanisms underlying its metabolic and physiological characteristics.

In contrast, LWLDP is characterized by the *PPP1R3B* gene, which is related to glycogen metabolism, and microbial taxa such as *Corynebacterium* and *Unidentified_Streptococcaceae*, which are associated with pathways involved in ascorbate and aldarate metabolism, starch and sucrose metabolism, and insulin signaling, all of which play critical roles in carbohydrate metabolism. Intestinal metabolites in the ileum, including apigenin 6,8-digalactoside, 3-[(Ethylanilino)methyl]benzenesulfonic acid, N-(5-chloro-2-hydroxyphenyl)-2-(phenylthio) acetamide, Progabide, and 16-phenoxytetranorprostaglandin F2α, as well as 5-keto-gluconic acid in the cecum, and metabolites in the rectum, such as 2-methyl-3-hydroxybutyric acid and Val-Asn, were linked to metabolites in the LD muscle, including CMP-N-acetylneuraminate, maltopentaose, mannose 6-phosphate, glucose 6-phosphate, 3,6-dichloro-N-(pyridin-2-ylmethyl)

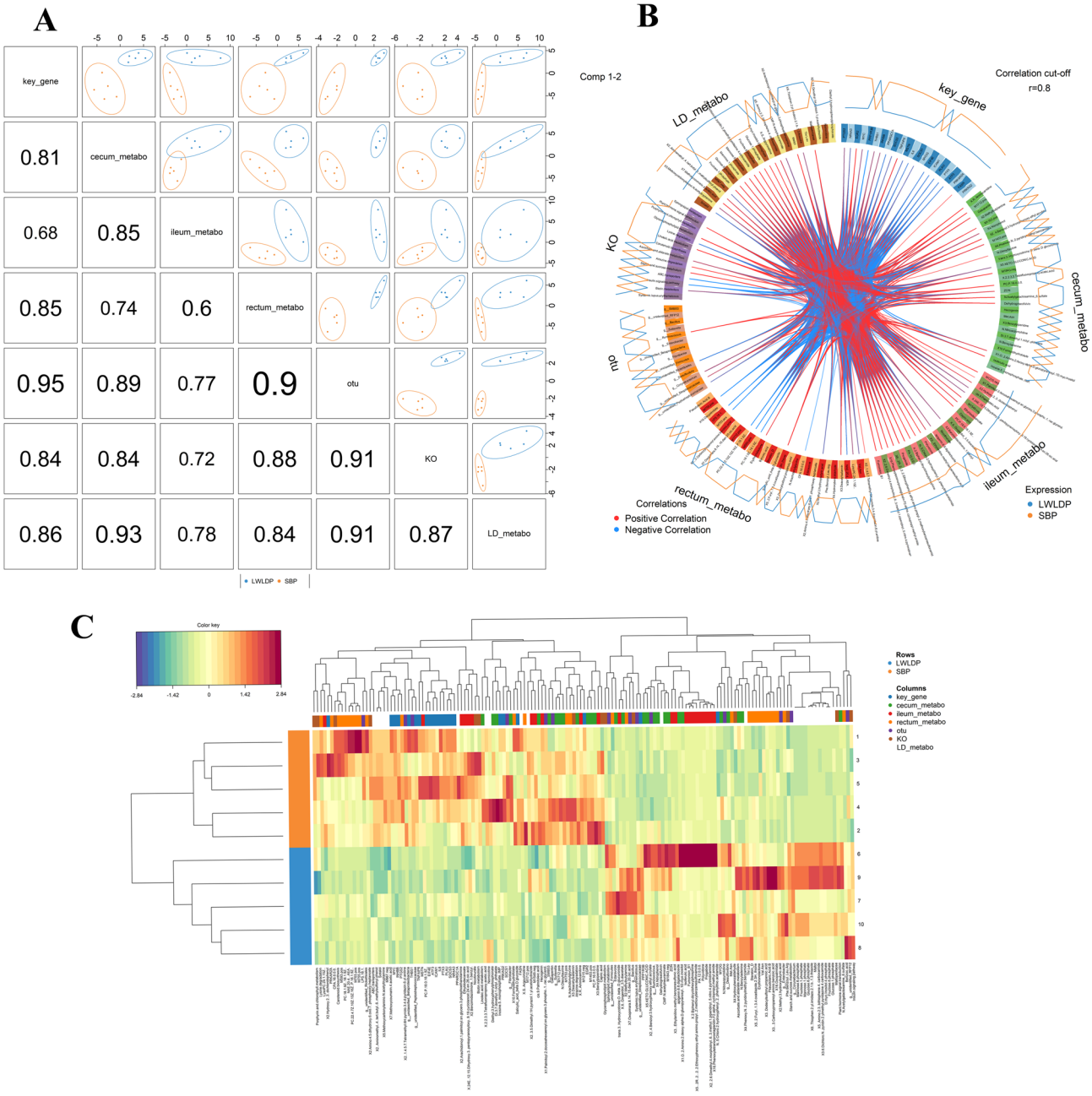

Fig. 6 Multiple omics integrative analysis for the seven kinds omics data of two breeds **(A)** Sample scatterplot made with plotDiablo, displaying the first component in the seven data set (upper diagonal plot) and the Pearson correlation between each component (lower diagonal plot) **(B)** Circos plot showing positive (yellow lines) and negative (blue lines) correlations ($r > 0.8$) between selected features from each dataset (feature names appear in each quadrant) **(B)** Clustered image map (Euclidean distance, Complete linkage) of the multi omics signature. Information from the ten pigs of two breed in the study are represented by rows, whereas selected features from each of the seven omics datasets are represented by columns (according to the color code line below the cladogram)

pyridazine-4-carboxamide, fructose 1-phosphate, mannose 6-phosphate, fructose 6-phosphate, glucose 1-phosphate, 5'-amino-2,3'-bithiophene-4'-carboxamide, and D-myo-inositol-4-phosphate (Fig. 7). These results provide comprehensive insights into the complex interplay between the gut microbiome, intestinal metabolites, and muscle-related genes, illustrating the unique metabolic signatures associated with SBP and LWLDP. The findings enhance our understanding of the molecular and metabolic networks governing fat deposition, meat quality, and carbohydrate metabolism in livestock.

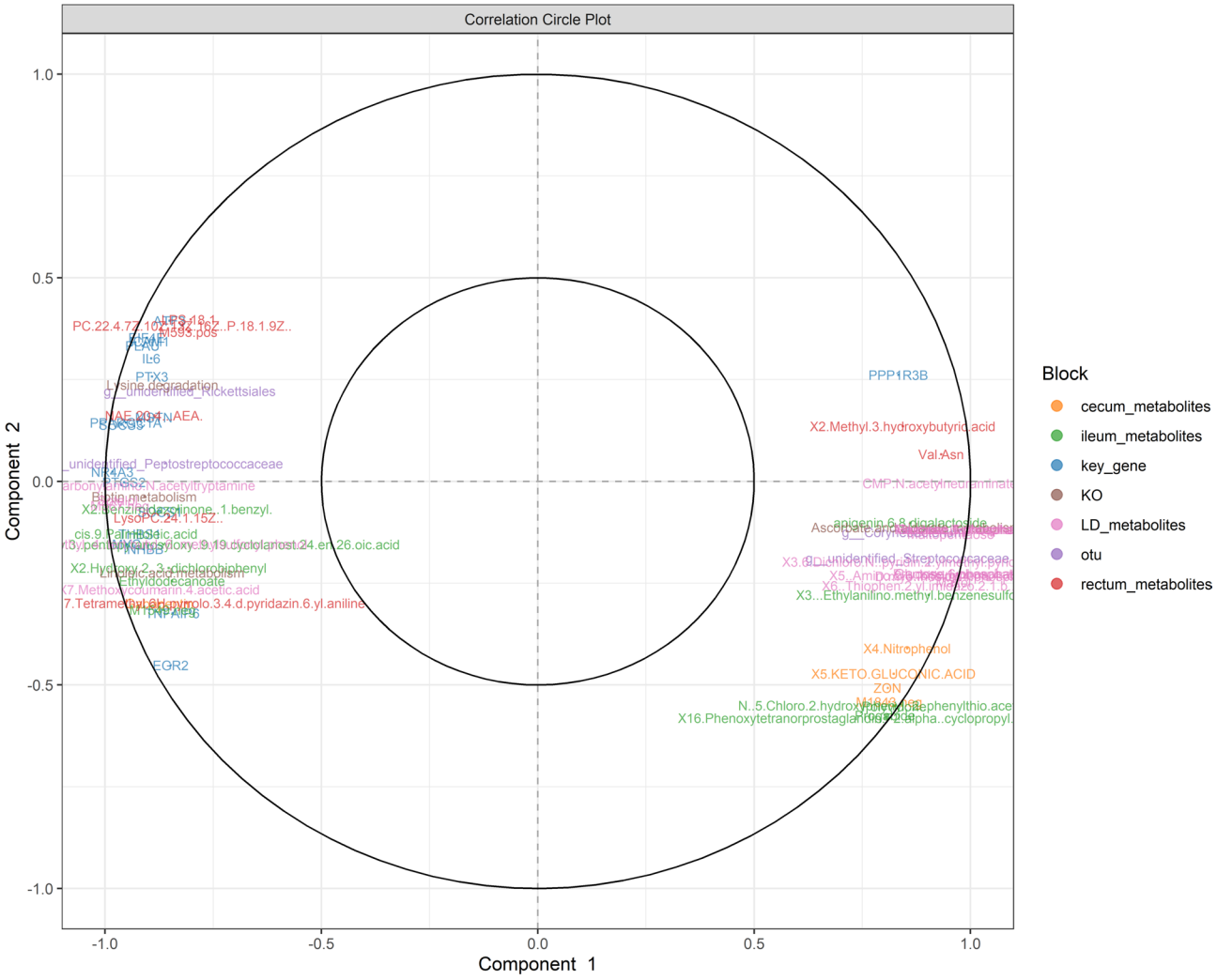

Fig. 7 The correlation circle plot showing relationships between seven types of omics data for both breeds. Variables with color-coded according to their respective omics blocks are displaying on the right side of the plot. The plot highlights variables that exhibit correlation at threshold of 0.8 across all seven omics layers

Discussion

Recent research is focusing on the crucial role of gut microbiota in host metabolism; however, the mechanisms underlying the gut-muscle axis and its influence on fat deposition and meat quality in pig breeds remain poorly understood. Our previous study demonstrated that Songliao Black Pig (SBP) exhibits superior meat quality traits, including higher marbling scores, increased back fat thickness, lower pH, enhanced meat color, reduced shear force, and lower drip loss compared to Large White × Landrace crossbred pigs (LWLDP). Fatty acid (FA) profiling identified fifteen significantly different FAs in LWLDP, with docosahexaenoic acid (DHA) was being more abundant in SBP. Integrative transcriptomic and metabolomic analyses further revealed key regulatory genes and metabolic pathways associated with fat deposition and meat quality in SBP. Notably, an imbalance in the insulin signaling pathway in LWLDP favored glycolysis over lipolysis, disrupting fat metabolism and compromising meat quality [30]. In the present study, we expanded on these findings by investigating gut microbiota composition and metabolite profiles across different intestinal regions and their relationship with key genes regulating fat deposition and meat quality. By integrating multi-omics data, our study provides novel insights into the gut-muscle axis and identifies potential microbial and metabolic biomarkers for improving pork quality.

Breed-specific gut microbial profiles and their functional implications

Gut microbiota analysis showed higher microbial abundance in the cecum and rectum of LWLDP compared to the ileum. *Firmicutes*, *Bacteroidetes*, *Proteobacteria*, and

Spirochaetes were the dominant phyla, consistent with previous study [44]. The *Lactobacillus* and *Streptococcus* abundant genera similarly aligned with previous findings [45]. Previous study reported that breed-specific differences in cecum and rectum are match with our findings [15, 24]. However, similar findings have been reported previously, in which *Lactobacillus* and *Bacteroides* were the dominant taxa [22]. These differences may reflect the unique physiological or metabolic requirements of each breed, affecting microbial colonization and diversity. This study found breed-specific differences in microbial composition. SBP cecum microbiota, enriched with fibroblastic and *Betaproteobacteria genera*, may enhance fiber degradation, supporting nutrient absorption in fiber-rich diets [46]. In contrast, LWLDP showed higher levels of *Corynebacterium*, *Unidentified_Desulfovibrio*, *UnidentifiedStreptococcaceae*, *Bacillus*, and *Enterobacter*, suggesting enhanced sulfur and amino acid metabolism, which may influence host metabolism and immune function [47, 48]. The rectum of SBP exhibited breed-specific with increased abundances of *Unidentified_Peptostreptococcaceae*, *Rickettsiales*, and *Sutterella*, *genera* associated with short-chain fatty acid (SCFA) production, which are important for gut health and energy balance [49]. In contrast, *Ruminococcus*, associated with polysaccharide degradation, was more abundant in LWLDP, suggesting that a microbiota composition that may enhance carbohydrate metabolism [50, 51]. These differences emphasize the role of microbial communities in meat quality, with each breed's microbiota influencing nutrient utilization and metabolic pathways. Understanding these variations can aid in improving breeding strategies and feed formulations to enhance meat quality. Breed-specific microbial pathways in the cecum of LWLDP are linked to starch and sucrose metabolism, sphingolipid metabolism, and immune regulation, indicating enhanced carbohydrate utilization and immune response [52]. The ABC transporter pathway was more enriched in SBP, indicating enhanced nutrient transport and environmental tolerance [53]. In the rectum, LWLDP showed increased pathways for insulin signaling, porphyrin and chlorophyll metabolism, and plant hormone signaling, supporting glucose metabolism and gut health [54, 55]. A greater abundance of ascorbate and aldarate metabolism, biotin metabolism, and linoleic acid metabolism pathways in SBP support vitamin and lipid biosynthesis and possibly enhance nutrient absorption and the oxidative stress response [56]. A low-linoleic acid diet has been shown to increase the conversion of ALA to DHA. This is achieved by upregulating the enzymes involved in fatty acid metabolism, specifically elongases and desaturases, which are crucial for the conversion processes [57]. Based on available findings of microbial taxa and metabolic pathways, our study is expressing, they are playing crucial role regulating the meat quality in pig breeds.

Microbial-metabolic pathways underlying meat quality and fat deposition in pigs

MixOmics analysis revealed that SBP is associated with key genes (*EIF4E*, *MSTN*, *PPARGC1A*, *NR4A3*, *SOCS1*, *THBS1*, and *INHBB*) linked to muscle and fat deposition. *Peptostreptococcaceae*, *Fibrobacter*, and *Rickettsiales* were associated with lysine degradation, biotin metabolism, and linoleic acid metabolism, influencing ileum and rectum metabolites like phospholipids, palmitoleic acid, gabapectin, and 2-benzimidazolinone. Muscle metabolites, such as 5-methoxycarbonylamino-N-acetyltryptamine and 7-methoxycoumarin-4-acetic acid, may regulate meat quality traits like marbling, drip loss, pH, and meat color. Previous studies have reported that *Peptostreptococcaceae* is associated with high-quality beef, suggesting its potential role in enhancing tenderness and intramuscular fat deposition. This highlights the intricate interplay between host genetics, gut microbiota, and metabolic pathways in determining meat quality [58]. The Tibetan pig is also known for its meat quality and has a relatively high abundance of *Bacteroides* and *Fibrobacterota* under semi-grazing conditions [59, 60]. Lysine degradation by gut microbes produces metabolites that can serve as biomarkers for meat quality, with altered levels potentially affecting livestock health and meat traits [61]. During lipid metabolism, PC (24:1) is catalyzed by phosphatidylcholine 2-acylhydrolase into PC (20:0/24:0), converted to PS (18:0/22:6), and further processed into PE via phosphatidylserine synthase [62]. PC (20:0/24:0) can produce long-chain fatty acids like arachidonic, calendic, and linoleate. Aspergillus, under certain conditions, can convert these into small metabolites like aldehydes and ketones, enhancing flavor [63]. Palmitoleic acid has been shown to improve metabolic health by reducing triglycerides and enhancing glucose metabolism. It acts as a lipokine, influencing systemic metabolism and potentially serving as an insulin-sensitizing agent [64]. Research indicates that it may also be involved in regulating lipogenesis, which is the process of converting carbohydrates into fatty acids, thereby playing a crucial role in energy homeostasis [64]. Previous studies showing that gut microbial species *B. uniformis*, *R. inulinivorans*, *B. vulgatus*, *C. catus*, *E. rectale*, and *F. prausnitzii* were all found to be positively correlated with the muscular metabolism-related genes including *MSTN*, *ATP2A1*, *MYLPF*, *ACTN3*, *MYL1*, and *TNNT3* and have positive effect on meat quality in cattle [27]. Obese Jinhua pigs had better meat quality that is associated with higher IMF content than lean Landrace pigs. To show that this trait was related to gut microbiota, mice were given microbiota from each pig species. The mice receiving Jinhua pig's

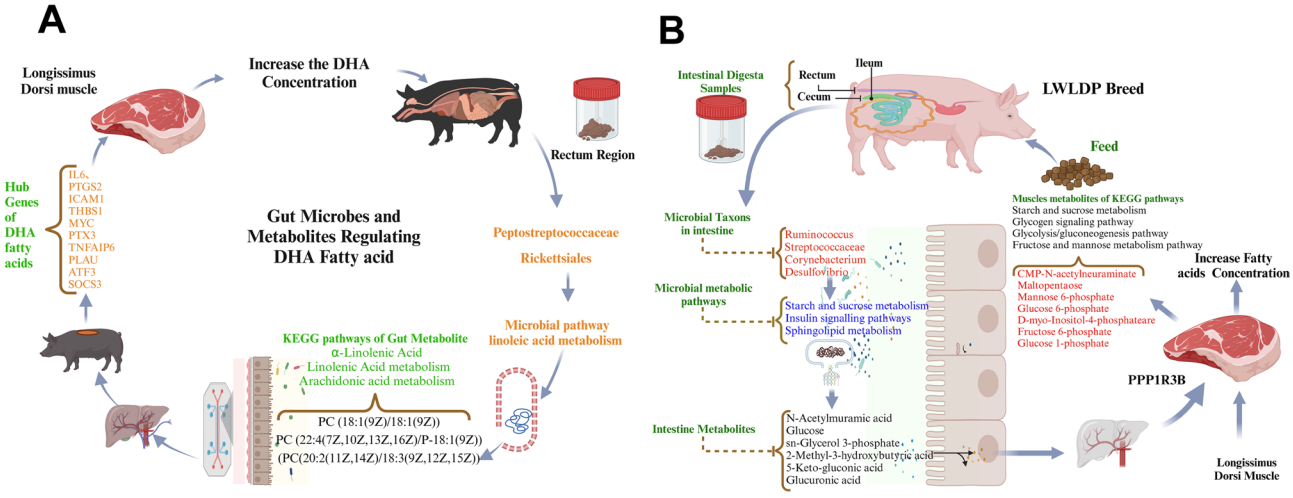

Fig. 8 **(A)** Showing the complex network of gut microbe and metabolites role in regulation fatty acids biosynthesis in longissimus dorsi muscle of LWLDP pig breed **(B)** Illustrates the complex network of gut microbe and metabolites role in biosynthesis of DHA fatty acid in longissimus dorsi muscle of SBP pig breed

microbiota had elevated lipid and triglyceride levels and the lipoprotein lipase activity, as well as reduced *ANGPTL4* expression in the muscle [28]. This increase was also accompanied with an elevated ratio of *Firmicutes/Bacteroidetes* and increased abundance of *Romboutsia. Prevotella copri*, and could increases fat accumulation by activating host chronic inflammatory responses through the TLR4 and mTOR signaling pathways. This also significantly upregulated the expression of the genes related to lipogenesis and fat accumulation (Fabp9, Scd1, Scd2, and Scd3) [29]. These integrated MixOmics results are showing that microbial taxa and metabolites may influence meat quality in pigs by producing small molecules and degrading various compounds, which can alter gene expression of meat quality and ultimately affect meat quality.

Gut microbial contributions to DHA enrichment and glycogen metabolism in pigs

The gut microbiota can influence the conversion of alpha-linolenic acid (ALA), a precursor of DHA, into its longer-chain forms through microbial linolenic acid metabolism [65]. We hypothesize that bacterial activity in the rectum, particularly within the linolenic acid and ALA pathways, may contribute to the higher muscle DHA concentration in SBP by modulating genes such *as IL6*, *PTGS2*, *ICAM1*, *THBS1*, *MYC*, and *SOCS3.* Previous research has linked bacteria from the *Peptostreptococcaceae* family to linoleic acid metabolism, producing beneficial fatty acids like conjugated linoleic acid (CLA) and vaccenic acid, which can influence tissue fatty acid profiles [66]. Additionally, the metabolite PC(22:4/18:1) can release arachidonic acid upon hydrolysis, serving as a precursor for eicosanoids involved in inflammation and cellular signaling [67]. Dietary ALA has been shown to alter gut microbiota composition and promote DHA synthesis, potentially through microbial modulation of linoleic and arachidonic acid metabolism [68]. This hypothesis is supported by the increased expression of DHA-associated genes observed in SBP (Fig. 8A). In contrast, LWLDP pigs presented increased abundances of key gut microbes and increased activity in metabolic pathways related to starch and sucrose metabolism, insulin signaling, and lipid metabolism. Intestinal and muscle metabolomic analyses revealed increased expression of gene involved in pathways linked to sugar metabolism, glycolysis, and glycogen storage. Our previous study revealed that the fatty acid concentrations of SFAs, MUFAs, PUFAs, and total fatty acids were much higher in LWLDP, along with PPP1R3B gene of insulin signaling pathway was correlated with maltopentaose, mannose 6-phosphate, glucose 6-phosphate, 3,6-dichloro-N-(pyridin-2-ylmethyl) pyridazine-4-carboxamide, fructose 1-phosphate, mannose 6-phosphate, fructose 6-phosphate, glucose 1-phosphate LD muscle metabolites [30]. Notably, we found that gut microbes in the cecum exhibit active metabolic pathways linked to starch and sucrose metabolism and the insulin signaling pathway, trends that align with the pathways associated with gut and muscle metabolites. We hypothesize that these gut microbes may modulate the expression of the PPP1R3B gene. This regulation may contribute to increased glycogen storage in muscle. The subsequent breakdown of stored glycogen via the glycolysis pathway could disrupt the balance between fat metabolism and catabolism. This imbalance might occur through microbial fermentation processes involving sucrose and mannose metabolism or the insulin signaling pathway in gut microbes (Fig. 8B). Our study concludes that gut microbes play a crucial role in regulating overall meat quality in pig breeds. SBP exhibits a unique

gut–muscle interaction that influences meat traits, while optimizing the gut microbial composition may enhance meat quality in the LWLDP breed.

Conclusion

In conclusion, our study provides valuable insights into the regulatory role of gut microbiota in pork quality through the gut-muscle axis. We found that cecum-associated microbes in LWLDP pigs enhance carbohydrate metabolism via insulin signaling and starch metabolism, potentially disrupting the balance between fat metabolism and catabolism. This shift favors glycolysis over lipolysis, leading to reduced fat deposition and lower meat quality. In contrast, rectum-associated microbes in SBP pigs contribute to DHA biosynthesis, supporting higher fat deposition and improved meat quality. These findings suggest that gut microbiota-derived metabolites could serve as biomarkers for optimizing pork production. However, further research needs to validate the regulatory mechanisms of gut microbiota in DHA biosynthesis, as well as the role of biomarkers along with controlled dietary interventions in enhancing the meat quality. Additionally, exploring breed-specific differences on a larger scale based on metagenomics will be crucial for a more comprehensive understanding of each active microbial pathway at species level and selection of crucial microbial pathways regulating meat quality may helpful in improving the meat quality. Future studies can also integrate the multiple omics data, such as proteomics, lipidomics, and transcriptomics, alongside gut microbiota and metabolites may provide deeper insights into metabolic pathways and open new directions for genetic selection, nutritional strategies, and microbiome-based interventions to improve pork quality and livestock breeding.

Abbreviations

LD	Longismuss dorsi
SBP	Songliao Black Pig
LWLDP	Large White × Landrace Pigs
DHA	Docosahexaenoic acid
UHPLC	Ultra-high-performance liquid chromatography
LA	Linoleic acid
ALA	α-linolenic acid
Val	Asn-Valine-Asparagine
PC	Phosphatidylcholine
NAE	N-Acylethanolamine
LysoPC	Lysophosphatidylcholine
DEGs	Differentially Expressed Genes
DEGs	Differentially Expressed Metabolites
GABA	Gamma-Aminobutyric Acid

Supplementary Information

The online version contains supplementary material available at https://doi.org/10.1186/s12866-025-04051-y.

Supplementary Material 1

Supplementary Material 2

Supplementary Material 3

Supplementary Material 4

Supplementary Material 5

Supplementary Material 6

Supplementary Material 7

Supplementary Material 8

Supplementary Material 9

Acknowledgements

Not applicable.

Author contributions

Conceptualization, S.T.K.; Methodology, S.T.K., Y.Z. (Yuan Zhao) and S.-M.Z.; Software, S.T.K.; Validation, S.T.K., Q.Z., R.M.A and Y.Z. (Yunpeng Zhang).; Formal Analysis, S.T.K.; Investigation, S.T.K., Q.Z. and Y.Z. (Yunpeng Zhang); Resources, Y.Z. (Yuan Zhao) and S.-M.Z.; Data Curation, S.T.K.; Writing—Original Draft Preparation, S.T.K.; Writing—Review and Editing, S.T.K., R.M.A., S.-M.Z., P.L., Z.J., Y.Z. (Yuan Zhao), W.-S.S.; Visualization, S.T.K.; Supervision, S.-M.Z., Y.Z. (Yuan Zhao); Project Administration, S.-M.Z. and Y.Z. (Yuan Zhao); Funding Acquisition, Y.Z. (Yuan Zhao)., Z.J., W.-S.S., and S.-M.Z. All authors have read and agreed to the published version of the manuscript.

Funding

This work was supported by the National Key Research and Development Program of China (2023YFF1001000), The National Natural Science Foundation of China (U21A20251), and The Key Technology Research and Development Program of Jilin Province of China (20240303075NC).

Data availability

The raw sequences of 16S rRNA has been uploaded to NCBI with Bio-Project Accession. No: PRJNA1173590.

Declarations

Ethics approval and consent to participate

All animal procedures were applied as per guidelines approved by the Institutional Animal Care and Use Committee (IACUC) of the Jilin Agricultural University. The study protocol was approved by the IACUC under approval number (KT2023023).

Consent for publication

Not applicable.

Competing interests

The authors declare no competing interests.

Author details

[1]Key Laboratory of Animal Production, Product Quality and Security, Ministry of Education, College of Animal Science and Technology, Jilin Agricultural University, Changchun 130118, China
[2]Institute of Animal Husbandry and Veterinary, Jilin Academy of Agricultural Sciences, Changchun 136100, China
[3]Jilin Provincial Engineering Research Center of Animal Probiotics, Jilin Provincial Key Laboratory of Animal Microecology and Healthy Breeding, Engineering Research Center of Microecological Vaccines (Drugs) for Major Animal Diseases, Ministry of Education, College of Animal Science and Technology, Jilin Agricultural University, 2888 Xincheng Street, Changchun 130118, China
[4]Key Laboratory of Grain and Oil Biotechnology, Academy of National Food and Strategic Reserves Administration, 11 Baiwanzhuang Avenue, Xicheng District, Beijing 100037, China

Received: 16 March 2025 / Accepted: 15 May 2025
Published online: 28 May 2025

References

1. Chernukha I, Kotenkova E, Pchelkina V, Ilyin N, Utyanov D, Kasimova T, Surzhik A, Fedulova L. Pork fat and meat: A balance between consumer expectations and nutrient composition of four pig breeds. Foods. 2023;12:690.
2. Wood J, Richardson R, Nute G, Fisher A, Campo M, Kasapidou E, Sheard P, Enser M. Effects of fatty acids on meat quality: a review. Meat Sci. 2004;66:21–32.
3. Kimura I, Ozawa K, Inoue D, Imamura T, Kimura K, Maeda T, Terasawa K, Kashihara D, Hirano K, Tani T. The gut microbiota suppresses insulin-mediated fat accumulation via the short-chain fatty acid receptor GPR43, nature communications. (2013);4:1829.
4. Parséus A, Sommer N, Sommer F, Caesar R, Molinaro A, Ståhlman M, Greiner TU, Perkins R, Bäckhed F. Microbiota-induced obesity requires farnesoid X receptor. Gut. 2017;66:429–37.
5. Yin J, Li Y, Han H, Ma J, Liu G, Wu X, Huang X, Fang R, Baba K, Bin P. Administration of exogenous melatonin improves the diurnal rhythms of the gut microbiota in mice fed a high-fat diet. Msystems. 2020;5:msystems101128–00002.
6. Icaza-Chávez M. Gut microbiota in health and disease. Revista De Gastroenterología De México (English Edition). 2013;78:240–8.
7. Jandhyala SM, Talukdar R, Subramanyam C, Vuyyuru H, Sasikala M, Reddy DN. Role of the normal gut microbiota. World J Gastroenterology: WJG. 2015;21:8787.
8. Yadav S, Jha R. Strategies to modulate the intestinal microbiota and their effects on nutrient utilization, performance, and health of poultry. J Anim Sci Biotechnol. 2019;10:1–11.
9. Lee JH, Kim S, Kim ES, Keum GB, Doo H, Kwak J, Pandey S, Cho JH, Ryu S, Song M. Comparative analysis of the pig gut Microbiome associated with the pig growth performance. J Anim Sci Technol. 2023;65:856.
10. Wen C, Wang Q, Gu S, Jin J, Yang N. Emerging perspectives in the gut–muscle axis: the gut microbiota and its metabolites as important modulators of meat quality. Microb Biotechnol. 2024;17:e14361.
11. Sebastià C, Folch JM, Ballester M, Estellé J, Passols M, García-Casco MuñozM, Fernández JM, Castelló AI, Sánchez A. A., Interrelation between gut microbiota, SCFA, and fatty acid composition in pigs, msystems. (2024);9:e01049–01023.
12. Zhao G, Xiang Y, Wang X, Dai B, Zhang X, Ma L, Yang H, Lyu W. Exploring the possible link between the gut microbiome and fat deposition in pigs, Oxidative Medicine and Cellular Longevity. (2022) 2022:1098892.
13. Zhu C, Yang J, Wu Q, Chen J, Yang X, Wang L, Jiang Z. Low protein diet improves meat quality and modulates the composition of gut microbiota in finishing pigs, frontiers in veterinary science. (2022) 9:843957.
14. Zhao W, Wang Y, Liu S, Huang J, Zhai Z, He C, Ding J, Wang J, Wang H, Fan W. The dynamic distribution of Porcine microbiota across different ages and Gastrointestinal tract segments. PLoS ONE. 2015;10:e0117441.
15. Ma J, Chen J, Gan M, Chen L, Zhao Y, Zhu Y, Niu L, Zhang S, Zhu L, Shen L. Gut microbiota composition and diversity in different commercial swine breeds in early and finishing growth stages. Animals. 2022;12:1607.
16. Li C, Zhao X, Zhao G, Xue H, Wang Y, Ren Y, Li J, Wang H, Wang J, Song Q. Comparative analysis of structural composition and function of intestinal microbiota between Chinese Indigenous Laiwu pigs and commercial DLY pigs. Veterinary Sci. 2023;10:524.
17. Gryaznova MV, Dvoretskaya YD, Syromyatnikov MY, Shabunin SV, Parshin PA, Mikhaylov EV, Strelnikov NA, Popov VN. Changes in the Microbiome profile in different parts of the intestine in piglets with diarrhea. Animals. 2022;12:320.
18. Morowitz MJ, Carlisle EM, Alverdy JC. Contributions of intestinal bacteria to nutrition and metabolism in the critically ill. Surg Clin. 2011;91:771–85.
19. Xie G, Zhang S, Zheng X, Jia W. Metabolomics approaches for characterizing metabolic interactions between host and its commensal microbes. Electrophoresis. 2013;34:2787–98.
20. Demain AL, Fang A. The natural functions of secondary metabolites, history of modern biotechnology I. (2000):1–39.
21. Roessner U, Dias DA. Metabolomics tools for natural product discovery. Springer; 2013.
22. Yang H, Huang X, Fang S, Xin W, Huang L, Chen C. Uncovering the composition of microbial community structure and metagenomics among three gut locations in pigs with distinct fatness. Sci Rep. 2016;6:27427.
23. Kelly J, Daly K, Moran AW, Ryan S, Bravo D, Shirazi-Beechey SP. Composition and diversity of mucosa-associated microbiota along the entire length of the pig Gastrointestinal tract; dietary influences, environmental microbiology. (2017) 19:1425–38.
24. Xiao Y, Kong F, Xiang Y, Zhou W, Wang J, Yang H, Zhang G, Zhao J. Comparative biogeography of the gut Microbiome between Jinhua and landrace pigs, scientific reports. (2018) 8:5985.
25. Yang H, Wu J, Huang X, Zhou Y, Zhang Y, Liu M, Liu Q, Ke S, He M, Fu H. ABO genotype alters the gut microbiota by regulating GalNAc levels in pigs. Nature. 2022;606:358–67.
26. Yin J, Li Y, Tian Y, Zhou F, Ma J, Xia S, Yang T, Ma L, Zeng Q, Liu G. Obese Ningxiang pig-derived microbiota rewires carnitine metabolism to promote muscle fatty acid deposition in lean DLY pigs. Innov. (2023) 4.
27. Zheng Y, Chen J, Wang X, Han L, Yang Y, Wang Q, Yu Q. Metagenomic and transcriptomic analyses reveal the differences and associations between the gut Microbiome and muscular genes in Angus and Chinese simmental cattle. Front Microbiol. 2022;13:815915.
28. Wu C, Lyu W, Hong Q, Zhang X, Yang H, Xiao Y. Gut microbiota influence lipid metabolism of skeletal muscle in pigs. Front Nutr. 2021;8:675445.
29. Chen C, Fang S, Wei H, He M, Fu H, Xiong X, Zhou Y, Wu J, Gao J, Yang H. Prevotella copri increases fat accumulation in pigs fed with formula diets. Microbiome. 2021;9:175.
30. Kumar ST, Zheng Y, Xu J, Zhao Z, Zhang Q, Zhang Y, Li M, Zou H, Azeem RM, Sun W-S. Transcriptome and Metabolome Insights into Key Genes Regulating Fat Deposition and Meat Quality in Pig Breeds, Animals. (2024);14:3560.
31. Wu J, Yang D, Gong H, Qi Y, Sun H, Liu Y, Liu Y, Qiu X. Multiple omics analysis reveals that high fiber diets promote gluconeogenesis and inhibit Glycolysis in muscle. BMC Genomics. 2020;21:660.
32. Li J, Zhang D, Yin L, Li Z, Yu C, Du H, Jiang X, Yang C, Liu Y. Integration analysis of metabolome and transcriptome profiles revealed the age-dependent dynamic change in chicken meat. Food Res Int. 2022;156:111171.
33. Smith C.A., Want E.J., O'Maille G., Abagyan R., Siuzdak G. XCMS: processing mass spectrometry data for metabolite profiling using nonlinear peak alignment, matching, and identification. Anal Chem. 2006;78:779–87.
34. Dunn WB, Erban A, Weber RJ, Creek DJ, Brown M, Breitling R, Hankemeier T, Goodacre R, Neumann S, Kopka J. Mass appeal: metabolite identification in mass spectrometry-focused untargeted metabolomics, Metabolomics. (2013);9:44–66.
35. Thevenot EA. Ropls: PCA, PLS (-DA) and OPLS (-DA) for multivariate analysis and feature selection of omics data. R Package Version. (2016);1.
36. Kolde R. pheatmap: Pretty Heatmaps. R package version 1.0. 12, 2019.
37. Tang D, Chen M, Huang X, Zhang G, Zeng L, Zhang G, Wu S, Wang Y. SRplot: A free online platform for data visualization and graphing. PLoS ONE. 2023;18:e0294236.
38. Ogata H, Goto S, Sato K, Fujibuchi W, Bono H, Kanehisa M. KEGG: Kyoto encyclopedia of genes and genomes, nucleic acids research. (1999);27:29–34.
39. Hall M, Beiko RG. 16S rRNA gene analysis with QIIME2, Microbiome analysis: methods and protocols. (2018):113–129.
40. Chen H, Boutros PC. VennDiagram: a package for the generation of highly-customizable Venn and Euler diagrams in R, BMC bioinformatics. (2011) 12:1–7.
41. Caspi R, Billington R, Fulcher CA, Keseler IM, Kothari A, Krummenacker M, Latendresse M, Midford PE, Ong Q, Ong WK. The metacyc database of metabolic pathways and enzymes, nucleic acids research. (2018) 46:D633–9.
42. Harrell FE, Dupont C. Hmisc: harrell miscellaneous, R package version. (2020) 4.
43. Rohart F, Gautier B, Singh A, Lê Cao K-A. MixOmics: an R package for 'omics feature selection and multiple data integration. PLoS Comput Biol. 2017;13:e1005752.
44. Crespo-Piazuelo D, Estellé J, Revilla M, Criado-Mesas L, Ramayo-Caldas Y, Óvilo C, Fernández AI, Ballester M, Folch JM. Characterization of bacterial microbiota compositions along the intestinal tract in pigs and their interactions and functions, scientific reports. (2018) 8:12727.
45. Liao SF, Nyachoti M. Using probiotics to improve swine gut health and nutrient utilization. Anim Nutr. 2017;3:331–43.
46. Pope P, Denman S, Jones M, Tringe S, Barry K, Malfatti S, McHardy A, Cheng J-F, Hugenholtz P, McSweeney C. Adaptation to herbivory by the Tammar wallaby includes bacterial and glycoside hydrolase profiles different from other herbivores, Proceedings of the National Academy of Sciences. (2010);107:14793–14798.
47. Zhang S, Zhang H, Zhang C, Wang G, Shi C, Li Z, Gao F, Cui Y, Li M, Yang G. Composition and evolutionary characterization of the gut microbiota in pigs. Int Microbiol. 2024;27:993–1008.
48. Ornelas A, Dowdell AS, Lee JS, Colgan SP. Microbial metabolite regulation of epithelial cell-cell interactions and barrier function, Cells. (2022);11:944.

49. Vital M, Karch A, Pieper DH. Colonic butyrate-producing communities in humans: an overview using omics data, Msystems. (2017);2:10.1128/msystems. 00130– 00117.
50. Ze X, Duncan SH, Louis P, Flint HJ. Ruminococcus bromii is a keystone species for the degradation of resistant starch in the human colon, the ISME journal. (2012);6:1535–43.
51. Sun Y, Zhou L, Fang L, Su Y, Zhu W. Responses in colonic microbial community and gene expression of pigs to a long-term high resistant starch diet. Front Microbiol. 2015;6:877.
52. Hannun YA, Obeid LM. Principles of bioactive lipid signalling: lessons from sphingolipids. Nat Rev Mol Cell Biol. 2008;9:139–50.
53. Davidson AL, Dassa E, Orelle C, Chen J. Structure, function, and evolution of bacterial ATP-binding cassette systems, microbiology and molecular biology reviews. (2008) 72:317–64.
54. Tremaroli V, Bäckhed F. Functional interactions between the gut microbiota and host metabolism. Nature. 2012;489:242–9.
55. Takeuchi T, Kubota T, Nakanishi Y, Tsugawa H, Suda W, Kwon AT-J, Yazaki J, Ikeda K, Nemoto S, Mochizuki Y. Gut microbial carbohydrate metabolism contributes to insulin resistance. Nature. 2023;621:389–95.
56. Peng L, Chen L, Wan J, Liu W, Lou S, Shen Z. Single-cell transcriptomic landscape of immunometabolism reveals intervention candidates of ascorbate and aldarate metabolism, fatty-acid degradation and PUFA metabolism of T-cell subsets in healthy controls, psoriasis and psoriatic arthritis. Front Immunol. 2023;14:1179877.
57. Kim D, Choi J-E, Park Y. Low-linoleic acid diet and oestrogen enhance the conversion of α-linolenic acid into DHA through modification of conversion enzymes and transcription factors. Br J Nutr. 2019;121:137–45.
58. Whon TW, Kim HS, Shin NR, Jung ES, Tak EJ, Sung H, Jung MJ, Jeong YS, Hyun DW, Kim PS. Male castration increases adiposity via small intestinal microbial alterations, EMBO reports. (2021) 22:e50663.
59. Niu H, Feng X-Z, Shi C-W, Zhang D, Chen H-L, Huang H-B, Jiang Y-L, Wang J-Z, Cao X, Wang N. Gut bacterial composition and functional potential of Tibetan pigs under semi-grazing. Front Microbiol. 2022;13:850687.
60. Chen B, Li D, Leng D, Kui H, Bai X, Wang T. Gut microbiota and meat quality. Front Microbiol. 2022;13:951726.
61. Driuchina A, Hintikka J, Lehtonen M, Keski-Rahkonen P, O'Connell T, Juvonen R, Kuula J, Hakkarainen A, Laukkanen JA, Mäkinen E. Identification of gut microbial lysine and histidine degradation and CYP-dependent metabolites as biomarkers of fatty liver disease, MBio. (2023) 14:e02663–02622.
62. Ecker J, Liebisch G. Application of stable isotopes to investigate the metabolism of fatty acids, glycerophospholipid and sphingolipid species, progress in lipid research. (2014) 54:14–31.
63. Novak M, Sepčić K, Kraševec N, Križaj I, Maček P, Anderluh G, Guella G, Mancini I. Targeted lipid analysis of haemolytic mycelial extracts of Aspergillus Niger, molecules. (2014) 19:9051–69.
64. Duckett SK, Volpi-Lagreca G, Alende M, Long NM. Palmitoleic acid reduces intramuscular lipid and restores insulin sensitivity in obese sheep, diabetes, metabolic syndrome and obesity: targets and therapy. (2014):553–63.
65. Todorov H, Kollar B, Bayer F, Brandão I, Mann A, Mohr J, Pontarollo G, Formes H, Stauber R, Kittner JM. α-Linolenic acid-rich diet influences microbiota composition and villus morphology of the mouse small intestine, Nutrients. (2020);12:732.
66. Devillard E, McIntosh FM, Duncan SH, Wallace RJ. Metabolism of Linoleic acid by human gut bacteria: different routes for biosynthesis of conjugated Linoleic acid. J Bacteriol. 2007;189:2566–70.
67. Sokoła-Wysoczańska E, Wysoczański T, Wagner J, Czyż K, Bodkowski R, Lochyński S. Patkowska-Sokoła B., Polyunsaturated fatty acids and their potential therapeutic role in cardiovascular system disorders—a review, Nutrients. (2018);10:1561.
68. Todorov H, Kollar B, Bayer F, Brandão I, Mann A, Mohr J, Pontarollo G, Formes H, Stauber R. α-Linolenic acid-rich diet influences microbiota composition and villus morphology of the mouse small intestine. Nutrients. 2020;12(3):732.

Publisher's note